

## Accepted Manuscript

The synthesis of hierarchical porous  $\text{Al}_2\text{O}_3$ /acrylic resin composites as durable, efficient and recyclable absorbents for oil/water separation

Xuejie Yue, Tao Zhang, Dongya Yang, Fengxian Qiu, Jian Rong, Jicheng Xu, Jiasheng Fang

PII: S1385-8947(16)31450-4  
DOI: <http://dx.doi.org/10.1016/j.cej.2016.10.049>  
Reference: CEJ 15904

To appear in: *Chemical Engineering Journal*

Received Date: 7 September 2016  
Revised Date: 12 October 2016  
Accepted Date: 13 October 2016

Please cite this article as: X. Yue, T. Zhang, D. Yang, F. Qiu, J. Rong, J. Xu, J. Fang, The synthesis of hierarchical porous  $\text{Al}_2\text{O}_3$ /acrylic resin composites as durable, efficient and recyclable absorbents for oil/water separation, *Chemical Engineering Journal* (2016), doi: <http://dx.doi.org/10.1016/j.cej.2016.10.049>

This is a PDF file of an unedited manuscript that has been accepted for publication. As a service to our customers we are providing this early version of the manuscript. The manuscript will undergo copyediting, typesetting, and review of the resulting proof before it is published in its final form. Please note that during the production process errors may be discovered which could affect the content, and all legal disclaimers that apply to the journal pertain.



**The synthesis of hierarchical porous Al<sub>2</sub>O<sub>3</sub>/acrylic resin  
composites as durable, efficient and recyclable absorbents for  
oil/water separation**

Xuejie Yue <sup>a</sup>, Tao Zhang <sup>a,b\*</sup>, Dongya Yang <sup>b</sup>, Fengxian Qiu <sup>a,b\*</sup>, Jian Rong <sup>a</sup>, Jicheng

Xu <sup>b</sup>, Jiasheng Fang <sup>c</sup>

<sup>a</sup> School of Chemistry and Chemical Engineering, Jiangsu University, Zhenjiang

212013, Jiangsu Province, China.

<sup>b</sup> Institute of Green Chemistry and Chemical Technology, Jiangsu University,

Zhenjiang 212013, Jiangsu Province, China.

<sup>c</sup> School of Chemistry and Chemical Engineering, Southeast University, Nanjing

211189, Jiangsu Province, China.

**Abstract:**

In this work, we report a facile and inexpensive approach which was demonstrated for the creation of hierarchical porous Al<sub>2</sub>O<sub>3</sub>/acrylic resin composites as durable, highly-efficient and recyclable absorbents for oil/water separation. Using hexadecyl trimethyl ammonium bromide (CTAB) as a structure-directing agent, the lamellar  $\gamma$ -AlOOH with porous architectures was successfully prepared via a hydrothermal route. The hierarchical Al<sub>2</sub>O<sub>3</sub> clusters, as the inorganic phase of resin

---

\*Corresponding authors:

Tel./fax: +86 511 88791800.

E-mail: zhangtaochem@163.com (T. zhang); fxqiu@126.com (F. Qiu)

composites, retain the unique structure of lamellar  $\gamma$ -AlOOH by calcination treatment.

In order to enhance the hydrophobic and oleophilic properties of  $\text{Al}_2\text{O}_3$  clusters, silane coupling agent (A151) was used to modify the surface of  $\text{Al}_2\text{O}_3$  clusters under microwave irradiation. The surface modified  $\text{Al}_2\text{O}_3$  clusters exhibit excellent hydrophobicity, oleophilicity and chemical stability, owing to the tight binding of the hydrophobic functional groups on the inorganic  $\text{Al}_2\text{O}_3$  clusters and the inherent stability of the grafted hydrophobic molecule chains. The porous  $\text{Al}_2\text{O}_3$ /acrylic resin composites were synthesized by suspension polymerization of butyl acrylate (BA) and methacrylic acid butyl ester (MBA) on the surface modified  $\text{Al}_2\text{O}_3$  clusters under microwave irradiation in the presence of coupling agents. The porous  $\text{Al}_2\text{O}_3$ /acrylic resin composites can effectively separate oils and organic solvents with high oil absorption rate and high oil retention capacity. Moreover, the obtained resin composites have high oil uptake capacities due to the synergy absorption of porous  $\text{Al}_2\text{O}_3$  clusters and acrylic resin. These excellent performances, such as excellent oil recoverability, excellent recyclability and high oil retention capacities, endow the material to be an ideal candidate to separate a variety of organic liquids from water.

**Keywords:** Oil absorption; acrylic resin; hierarchical porous  $\text{Al}_2\text{O}_3$ ; resin composites; suspension polymerization

## 1. Introduction

With the rapid development of modern science and the industrialized world, the demand for oils and organic solvents is sharply increasing. However, oils and organic solvents can cause environmental pollution during production, transportation, storage,

refining and usage [1-3]. For the local ecology system, the leaking oil floating on the water surface acts as a destroyer to smother underneath living organisms by blocking the air transfer and destroys the organizational structure of seabird feathers which are lipophilic [4, 5]. The detriment especially causes great harm to the marine aquaculture and negative economic impacts on tourism [5-7]. Therefore, the water pollution crisis due to the increasing release of wastewater containing oils and organic solvents into the environment is a challenge which exigently needs to develop an adequate and efficient process for removing these oils.

Enormous studied by researchers of various countries during the past decade have been done and many approaches have been devoted to removal the oils and organic solvents from water, such as chemical [8, 9], biological methods [10] and mechanical [11, 12]. Because the oil is composed mainly of alkane, which is difficult to participate in chemical reactions, the chemical methods including *in situ* burning and solidification have to solve the pollution of oil spill indirectly. However, the secondary pollution cannot be ignored due to the combustion and solidification products of oils to the environment [13]. With regard to biological method, it is a clean technology with the advantages of being environmentally safe, cost-effective, and does not generate secondary waste. However, the floating oils is hardly biodegraded by aquatic microbial communities; on the other hand, researchers use the special microorganism to degrade pollution, but in order to maintain the proliferation of microorganisms, it requires rigorous condition, because many variables restrict the use of microorganism, such as the accessibility of the pollution to the microorganism,

the optimization of biological activity and the inherent biodegradability of the pollution [14]. Hence, biological method has some disadvantages which limit its application on biodegradation of oils. Mechanical method commonly uses oil booms, barriers, and skimmers to clean up oil spills or organic pollution. However, the oils or organic solvents cannot be removed completely by those devices with the intrinsic hydrophilic property and low absorption selectivity [15]. More importantly, these approaches have limitations in poor efficiency. Alternatively, the absorption technology has been regarded as the one of the most promising technologies to these points [16, 17]. A large number of traditional materials have been used widely to absorb oil spilled water, including clay [18], activated carbon [2], polymeric fiber [19] and waste barley straw [20]. These materials with facile operation, low energy consumption, low cost and wide origin have a lot of disadvantages, such as poor separate selectivity, low absorption capacity, low oil absorption rate, difficulty to recover, etc. [21]. Therefore, it is essential to search for a new style of oil absorption materials that overcome these disadvantages.

Inspired by the high water absorption resin, a super oil absorption acrylic resin can overcome these defects due to oil-swelling properties. Acrylic resin is crosslinked copolymer with low crosslinking degree and a three-dimensional (3D) network structure that owns many good properties [22], including high selectivity, low cost, convenient recovery and resistance to water and it has crosslinked 3D hydrophobic network formed by monomers, which is one of the most characteristic features [23]. In emergencies, the faster rate of oil absorption and the higher capacity of oil

absorption are meaningful properties and 3D net structure of the resin plays a leading role in these performances [24]. However, these traditional acrylic resins have slow oil absorption rate and low oil absorption capacity and the defects of acrylic resins themselves cannot be ignored. Many oil-absorption resins have been designed to improve the general structure of the oil-absorption resin, reduce the crosslinked network of space resistance and enhance mechanical properties. For instance, Atta et al. [23] selected a novel monomer cinnamoyloxyethyl methacrylate to copolymerize with isooctyl acrylate and determining the influence of monomer on the absorption capacity. Experiments draw a conclusion that the oil absorbency was increased by incorporation of hydrophobic acrylate units and by decreasing the amount of either crosslinking agent. Zhou et al. [25] chose flexible macromolecular ethylene-propylene-diene terpolymer and rigid molecule styrene as monomers and the best oil absorptivity of the resin was about 11.5 g/g in diesel. Shan et al. [26] used polybutadiene as crosslinker to form a kind of relaxing network with both a high gel fraction and low crosslink density and the resin achieved high oil absorptivity of 14 g/g in benzene.

It is widely known that inorganic nanomaterials have a great influence on polymer properties and organic-inorganic resin composites could combine the advantages of the inorganic material and the organic material because of synergistic effect by them [27]. The hierarchical porous  $\text{Al}_2\text{O}_3$  obtained by calcining the precursor  $\text{AlOOH}$  is a typical functional nanomaterial, which plays an important role in industry because of its specific surface areas, high porosities, low densities and porosity

[28-30]. Because of the well dispersion of the hierarchical  $\text{Al}_2\text{O}_3$  in the polymer matrix and the interfacial interaction between the inorganic and organic phases, the  $\text{Al}_2\text{O}_3$  resin composites have been significantly improved in the thermal stability and mechanical properties. Moreover, the porous structures weaken the net of polymer chains entanglement and decrease the crosslink density of resin, thereby the absorption capacity and the oil absorption rate are improved, which is extremely important in emergency treatment of oil leakage [29].

Herein, we describe the synthesis of porous  $\text{Al}_2\text{O}_3$ /acrylic resin composites by suspension polymerization method and characterization of hierarchical porous  $\text{Al}_2\text{O}_3$  nanomaterial using CTAB as a structure-directing agent. The synthesized composites benefit from the introduction of chemical bonds between inorganic and organic phases exhibit excellent oil-absorbing properties, high oil absorption capacity and good reusability of oil-absorbing resins, which have promising application in the treatment of oil leakage.

## 2. Materials and methods

### 2.1. Materials

BA, MBA, ethyl acetate (EA), N,N'-methylene diacrylamide, polyvinyl alcohol (PVA), carbon tetrachloride ( $\text{CCl}_4$ ), toluene, anhydrous ethanol, trichloromethane ( $\text{CCl}_3$ ), CTAB and aluminum nitrate nonahydrate ( $\text{Al}(\text{NO}_3)_3 \cdot 9\text{H}_2\text{O}$ ) were purchased from Sinopharm Chemical Reagent Co.,Ltd. Triethoxyvinylsilane (A151,  $\geq 97\%$ ) was purchased from Shanghai Macklin Biochemical Co.,Ltd. All above agents were of analytical grade and used without further purification. Benzoyl peroxide (BPO)

supplied by Sinopharm (Shanghai, China) was dissolved in the  $\text{CCl}_3$  and precipitated by the addition of ethanol. The obtained precipitate was dried in a vacuum oven at  $60\text{ }^\circ\text{C}$  prior to use.

## 2.2. Preparation of hierarchical porous $\gamma\text{-Al}_2\text{O}_3$

The precursor  $\text{AlOOH}$  was prepared according to the method reported previously [31]. In a typical synthesis, 10 mmol of  $\text{Al}(\text{NO}_3)_3 \cdot 9\text{H}_2\text{O}$  and 4 mmol of CTAB were dissolved in deionized water, and the mixture were under magnetic stirring for 0.5 h. The obtained transparent solution was transferred to Teflon-lined, stainless-steel autoclave, and it would be placed into an oven at  $180\text{ }^\circ\text{C}$  for 12 h. The colloidal product was centrifuged and washed three times with deionized water, followed by anhydrous ethanol two times. Then, the precursor  $\text{AlOOH}$  was dried at  $55\text{ }^\circ\text{C}$  in vacuum for 12 h. Finally, the precursor  $\text{AlOOH}$  was calcimined at  $500\text{ }^\circ\text{C}$  for 3 h in the air and the hierarchical porous  $\text{Al}_2\text{O}_3$  was obtained.

## 2.3. Surface hydrophobic modification of porous $\text{Al}_2\text{O}_3$

The chunk  $\text{Al}_2\text{O}_3$  was grinded with an agate mortar. 3.0 g of  $\text{Al}_2\text{O}_3$  was dispersed into 100 ml alcohol aqueous solution (volume ratio of alcohol to deionized water is 1:1). Then 1.5 g of A151 solution was dropped to the  $\text{Al}_2\text{O}_3$  suspension slowly. The mixtures were sealed and placed in the microwave reaction system with a frequency of 2.45 GHz. The reaction system was rapidly heated to  $85\text{ }^\circ\text{C}$  at a power of 700 W, and maintained at  $85\text{ }^\circ\text{C}$  for 3 h with rotation and magnetic stirring. Finally, the modified porous  $\text{Al}_2\text{O}_3$  nanomaterial for next experiment was washed several times and dried in vacuum oven at  $80\text{ }^\circ\text{C}$  for 24 h.



#### 2.4. Preparation of resin composites

The resin composites were prepared by suspension polymerization. In a typical synthesis, 1 g of PVA was dissolved with 20 ml deionized water in a three-neck flask with a magnetic stirring at 90 °C for 30 minutes. The mixed solution, containing modified porous Al<sub>2</sub>O<sub>3</sub>, 4 g of BA, 6 g of MBA and 5 g of EA were added into the PVA aqueous solution. The mixed solution was further stirred for 20 minutes to disperse the surface modified porous Al<sub>2</sub>O<sub>3</sub>. 0.18 g of N,N'-methylene diacrylamide dissolved in the 10 ml of deionized water was added dropwise into the emulsion. After polymerization at 60 °C for 20 min, 70 °C for 20 min and 80 °C for 90 min, obtained porous Al<sub>2</sub>O<sub>3</sub>/resin composites was washed by anhydrous ethanol several times. Finally, the resin was dried in a vacuum oven at 60 °C for 24 h. Depending on the different weight ratio of the porous Al<sub>2</sub>O<sub>3</sub> and monomers, a series of porous Al<sub>2</sub>O<sub>3</sub>/acrylic resin composites with different porous Al<sub>2</sub>O<sub>3</sub> clusters loadings were prepared.

#### 2.5. Sample characterization

The morphologies of the AlOOH clusters, raw acrylic resin and porous Al<sub>2</sub>O<sub>3</sub>/acrylic resin were analyzed by JSM-6010 SEM (JEOL, Japan). The SEM specimens were prepared by sputter coating a thin gold layer approximately 3 nm thick. X-ray diffraction (XRD) analysis was employed to identify the crystallography of Al<sub>2</sub>O<sub>3</sub> and AlOOH. The XRD analysis was performed using Shimadzu XRD-6100 instrument with Cu K $\alpha$  radiation at 40 kV and 30 mA, a scanning rate of 4°/min, and a 2 theta angle ranging from 10° to 80°. To detecting the functional groups and

chemical structure, Fourier transform infrared spectroscopy (FT-IR) spectrometer analysis was performed using a Nicolet Nexus 470 FT-IR spectrometer with resolution  $4\text{ cm}^{-1}$  operating in the range of  $4000\text{--}450\text{ cm}^{-1}$  via potassium bromide (KBr, optical grade) pellet. Thermogravimetric analysis (TGA) and differential scanning calorimetry (DSC) were carried out simultaneously using a STA 449C instrument (NETZSCH Corporation, Germany) with the heating rate of  $10\text{ }^{\circ}\text{C}/\text{min}$  under nitrogen atmosphere. The water contact angle measurement was carried out by applying  $5\text{ }\mu\text{L}$  of deionized water and at least three different spots on the same sample surface were taken for contact angle measurements to receive a mean value. Surface properties of the porous  $\text{Al}_2\text{O}_3$  were studied by the Brunauer-Emmett-Teller (BET) methods via nitrogen adsorption and desorption measurements.

#### 2.6. Oil absorption experiment

The oil absorption capacity was performed at  $25\text{ }^{\circ}\text{C}$  and measured by the gravimetric method. The resin composites were weighed and immersed into the organic solvents for 10 h. After that, the sample was taken out from liquid and weighted immediately. Each oil absorption experiment was repeated three times and took the average. The oil absorption properties of absorbent sample were calculated by the following formula:

$$Q_{\text{eq}}(\text{g/g}) = (m_e - m_o) / m_o \quad (1)$$

Where  $Q_{\text{eq}}(\text{g/g})$  is the sorption capacity of the absorbent,  $m_e(\text{g})$  is the weight at equilibrium, and  $m_o(\text{g})$  is the intimal weight of the absorbent.

#### 2.7. Recovery of the oil-absorbing resins

To test the regeneration capacity of porous  $\text{Al}_2\text{O}_3$ /acrylic resin composites, the saturated oils and organic solvents were recovered by a method of extraction with anhydrous ethanol three times, followed by vacuum drying at  $80\text{ }^\circ\text{C}$  for 12 h. The process was repeated five times to confirm the reusability of porous  $\text{Al}_2\text{O}_3$ /acrylic resin composites. For each cycle, the composites were weighed before and after oils absorption.

### 3. Results and discussion

#### 3.1 Structure and morphology analysis of hierarchical porous $\gamma\text{-Al}_2\text{O}_3$

The hydrothermal and calcination influenced the morphology of obtaining materials and the morphology of the as-prepared samples were examined by powder XRD. The XRD results of raw and calcined  $\gamma\text{-AlOOH}$  are illustrated in Fig.1, indicating that the calcination treatment lead to the change of structure of  $\gamma\text{-AlOOH}$  and the transformation of the phase from boehmite to amorphous  $\gamma\text{-Al}_2\text{O}_3$ . Fig.1a shows the XRD pattern of the prepared  $\text{AlOOH}$  powder. The diffraction peaks at  $10 < 2\theta < 80^\circ$  were indexed as reflections of (020), (120), (031), (051), (002) and (251) crystal planes of orthorhombic  $\gamma\text{-AlOOH}$  (JCPDS card no. 83-2384) and were assigned to be the boehmite phase, indicating that crystalline boehmite phase  $\text{AlOOH}$  was obtained under the hydrothermal conditions. Additional diffraction peak is indicated with asterisk; it most likely results from  $\text{Al}(\text{OH})_3$  produced by the hydrolysis of  $\text{Al}(\text{NO}_3)_3$  and a small amount of  $\text{Al}(\text{OH})_3$  did not translate into  $\text{AlOOH}$ , because the  $\gamma\text{-AlOOH}$  was formed by dehydrating the  $\text{Al}(\text{OH})_3$  [32]. Fig.1b shows a typical diffraction pattern of  $\gamma\text{-Al}_2\text{O}_3$  obtained by calcining  $\gamma\text{-AlOOH}$  at  $500\text{ }^\circ\text{C}$  for 3 h in

the air. All the diffraction peaks were assigned to the diffraction from (111), (311), (222), (400) and (440) crystal planes of cubic structure of  $\gamma$ - $\text{Al}_2\text{O}_3$  and they were in good agreement with the standard values (JCPDS card no.79-1558). No other impurity phases were detected, which not only indicted the product is high quality, but also indicted the disappearance of the additional diffraction peak in the Fig.1a. The disappearance of the additional diffraction peak indirectly proved the additional diffraction was ascribed to  $\text{Al}(\text{OH})_3$ , which transformed to  $\gamma$ -alumina by calcination. The weak and broad diffraction peaks indicate the samples are composed of small crystals with a crystalline size in nanometer scale [33]. Thus, the boehmite structure transformed to  $\gamma$ -alumina after calcination at 500 °C. No other impurity phases were detected, indicating  $\gamma$ - $\text{Al}_2\text{O}_3$  is of high quality.

The morphology and structural characterizations of the lamellar  $\text{Al}_2\text{O}_3$  architectures are analyzed by scanning electron microscopy. Fig.2A and B show the panoramic and the magnified images, respectively, of the  $\text{Al}_2\text{O}_3$  architectures. The samples display large quantities of uniform, lamellar structures and the sheets build  $\gamma$ - $\text{Al}_2\text{O}_3$  ellipsoidal particles, which possess the nanosheet lengths in the range of 2-3  $\mu\text{m}$  with a regular cluster structure and the thickness of about 88 nm (Fig.4B). The unique lamellar structure of  $\text{Al}_2\text{O}_3$  is formed with the help of CTAB micelle molecules [34]. CTAB can ionize completely and a surfactant film can form a covering film on the newly generated amorphous  $\text{Al}(\text{OH})_3$  to reduce the interface energy. In the crystallization process, the preferential adsorption of  $\text{CTA}^+$  head groups facilitate uniform the form of  $\text{AlOOH}$  lamellar architectures with a preferential

growth direction under hydrothermal condition. Then,  $\text{Al}_2\text{O}_3$  ellipsoidal particles retain the unique architecture of  $\text{AlOOH}$  by calcination. The hierarchical  $\text{Al}_2\text{O}_3$  clusters are further demonstrated in Fig.2B. It is clearly that  $\text{Al}_2\text{O}_3$  nanosheet stock together loosely, because CTAB may serve as not only a growth, but also an agglomeration inhibitor. The fluffy structures provide more space and channels for oil absorption to improve the resin composites.

As an important type of functional nanomaterial, porous  $\text{Al}_2\text{O}_3$  clusters has been used as an absorbent with large specific surface area, high porosity, which are beneficial to oils and organic solvents absorption. The  $\text{N}_2$  adsorption and desorption isotherms, combining the pore size distribution (inset) for  $\text{Al}_2\text{O}_3$  obtained after a calcination of  $500\text{ }^\circ\text{C}$  are shown in Fig.3. The surface area is calculated by the Brunauer–Emmett–Teller (BET) method and the pore size is obtained from the pore size distribution curve calculated by the Barrett–Joyner–Halenda (BJH) method. The pore volumes are estimated from the amount adsorbed at a relative pressure of  $\sim 0.99$ . As shown in Fig.3, the isotherms of  $\text{Al}_2\text{O}_3$  show a gradual uptake at low pressure followed by a steep uptake at higher pressure and confirm the porous property of  $\text{Al}_2\text{O}_3$ . Desorption occurs with a hysteresis in the  $P/P_0$  range of  $0.43\text{--}0.95$ . After calcination, the  $\text{Al}_2\text{O}_3$  has a high (BET) specific surface area of  $238.8\text{ m}^2/\text{g}$  and the total pore volume is found to be  $0.50\text{ cm}^3/\text{g}$  at  $P/P_0\ 0.99$ . Interestingly, there are several types of mesopore existing in the  $\text{Al}_2\text{O}_3$  clusters (see inset of Fig.3). Two types pore size distribution are  $3\text{--}4\text{ nm}$  and  $4\text{--}7\text{ nm}$ , respectively, which may come from the mesoporous  $\text{Al}_2\text{O}_3$  clusters. The porous lamella structure of  $\text{Al}_2\text{O}_3$  is favorable to

efficient improve the oil-absorbing properties of resin composites, because the unique structure is beneficial to oils and organic solvents transport and absorption.

### 3.2 Surface hydrophobic modification of $\text{Al}_2\text{O}_3$ clusters

Wettability of hierarchical  $\text{Al}_2\text{O}_3$  clusters to water is one of the most important considerations when selecting suitable adsorbent for oils and organic solvents absorption. To test the hydrophobic nature of the prepared  $\text{Al}_2\text{O}_3$  powder and the surface-modified  $\text{Al}_2\text{O}_3$  powder, contact angle measurements were performed using sessile drop method with water. For the measurements, the powder was compressed on the surface of a glass slide. As shown in Fig. 4A, when deionized water droplet was dropped onto the surface of  $\text{Al}_2\text{O}_3$ , it was completely spread out on the surface of unmodified  $\text{Al}_2\text{O}_3$  suggesting the hydrophilic character. On the contrary, in Fig. 4B, the modified  $\text{Al}_2\text{O}_3$  retained the water droplet on its surface, indicating its high hydrophobic character with static contact angle of  $145.49^\circ$ . In addition, it was observed that the dynamic absorbing process of water on the modified  $\text{Al}_2\text{O}_3$  (Fig.5) within 30 s, which showed the efficient hydrophobic property of the modified  $\text{Al}_2\text{O}_3$ . With increasing time of contact with the modified  $\text{Al}_2\text{O}_3$ , the water droplet did not sink in the powders. The modified  $\text{Al}_2\text{O}_3$  excellent hydrophobic property may likely be a consequence of the hydrophobic functional group induced by the A151 organosilicone coating. Under an ethanol water system, the surface modification was assumed to proceed via following two steps: (□) hydrolysis of the A151 generated -Si-OH groups; and (□) the dehydration reactions between hydroxyl groups. The dehydration reaction between the -Si-OH groups and hydroxyl groups of hierarchical

$\text{Al}_2\text{O}_3$  clusters formed an organosilicone coating including double carbon bonds on the hierarchical  $\text{Al}_2\text{O}_3$  clusters (as shown in Scheme 1).

Successful surface modification of  $\text{Al}_2\text{O}_3$  clusters was further demonstrated. Fig. 6A and B shows the FT-IR spectra of the unmodified and modified  $\text{Al}_2\text{O}_3$  clusters by A151, respectively. The characteristic absorption peaks in the two curves nearby at  $3460\text{ cm}^{-1}$  and  $1633\text{ cm}^{-1}$  were assigned to the  $-\text{OH}$  bands absorption of typical spectrum of  $\text{H}_2\text{O}$ . In  $400\text{-}1000\text{ cm}^{-1}$  wave number range of two curves had a broad absorption band, which is the characteristic absorption band of the Al-O bond [36]. Compared with the absorption peak of the unmodified  $\text{Al}_2\text{O}_3$  (Fig.6A) at  $1390\text{ cm}^{-1}$ , the absorption peak of the  $\text{Al}_2\text{O}_3$  modified by A151 (Fig.6B) became sharp and weak, which indicated the decrease of hydroxyl group content and polarity on the surface of  $\text{Al}_2\text{O}_3$  clusters. In addition, the absorption peak of unmodified  $\text{Al}_2\text{O}_3$  at  $1515\text{ cm}^{-1}$  disappeared in the Fig.6B. The main reason may alkoxy of A151 hydrolyze to form silanol and take place condensation reaction with hydroxyl groups on the surface of the  $\text{Al}_2\text{O}_3$  (Scheme 1). The weak and sharp absorption peak at  $1610\text{ cm}^{-1}$  and  $1278\text{ cm}^{-1}$  (Fig. 6B) can be ascribed to the C=C bending vibration and the Si-C bending vibration of silane coupling agent, indicating the presence of organosilicone coating and the modification of  $\text{Al}_2\text{O}_3$  by A151 successfully.

### 3.3 Preparation of porous resin composites

As an important type of functional nanomaterial,  $\text{Al}_2\text{O}_3$  has been used as an absorbent with special hierarchical structures to improve the inner structure of resin composites, which are beneficial to oils and organic solvents absorption. Fig.7A and

B reveal the structures of raw acrylic resin and the resin composites at the same magnification, respectively. It is shown that the surface of the resin is smooth with a small amount of protrusions in Fig.7A. Some gaps in the surface of the resin are formed during the polymerization of the monomers to the three dimensional hierarchical structure and the gaps are favorable to improve the oil-absorbing rate. In comparison with raw acrylic resin, the surface of the resin composites (Fig.7B) is rather rougher than the raw resin because of the involvement of the modified hierarchical  $\text{Al}_2\text{O}_3$  clusters during the polymerization of the monomer. In the process of synthesizing resin composites, the double carbon bonds of BA, MBA and the organosilicone coating of the modified  $\text{Al}_2\text{O}_3$  clusters were transformed into free radicals under a microwave field, and with the help of free radical polymerization, a chain was initiated. At last, the bending and entangling of chains formed the 3D network structure, meanwhile the modified  $\text{Al}_2\text{O}_3$  clusters were enveloped inside the chains (as shown in Scheme 2). In addition, it should be noted that several holes were observed on the surface of the resin composites, which is favorable to efficient improved the oil-absorbing properties of resin composites.

The influence of hierarchical porous  $\text{Al}_2\text{O}_3$  clusters on the thermal stability of acrylic resin was investigated by TGA under nitrogen atmosphere. Each sample was first heated to 200 °C to ensure standardized removal of residual water and solvents. The TG-DSC curves of acrylic ester resin and porous  $\text{Al}_2\text{O}_3$ /acrylic resin composites are showed in Fig.8. As shown in Fig.8A and B, the onset of a low and steady thermal degradation process of two samples is found to occur until rapid decomposition and a



rapid phase of mass loss appeared at 331-413 °C and 338-462 °C (Weight retention from 90% to 10%), respectively, which indicated that the thermal stability of resin composites had been improved because of synergistic effect of acrylic resin and hierarchical Al<sub>2</sub>O<sub>3</sub> clusters. Each of TG-curves shows only one degradation stage, which is attributed to random chain scission of the resin. Moreover, the residue weight of acrylic ester resin is 3.22 wt%, owing to the residual carbon after the decomposition of the resin under nitrogen atmosphere; the residue weight of porous Al<sub>2</sub>O<sub>3</sub>/acrylic resin composites is 9.23 wt%, owing to the residue carbon of resin and the doped Al<sub>2</sub>O<sub>3</sub> clusters. The DSC results of acrylic resin show that there are two endothermic peaks of acrylic resin at 391 °C and 757 °C. The 95.1 % weight loss from 227 °C to 452 °C is because of the decomposition of the acrylic resin with the exothermic peak at about 391 °C. Compared with acrylic resin, the resin composites show a similar DSC curve and it loses 86.2 % weight from 255 °C to 477 °C. Interestingly, resin composites show a same endothermic peak at 391 °C and has a much broader and higher endothermic peak at 932 °C than the endothermic peak of acrylic resin at 757 °C. After the endothermic peak at 391 °C, the two samples decompose the remaining part products of resin and form the second endothermic peak. But, the crystal transition of Al<sub>2</sub>O<sub>3</sub> in the resin composites from  $\gamma$ -phase to  $\alpha$ -phase may be attributed to form the broader and higher endothermic peak at 932 °C [37].

#### 3.4. Absorption properties of resin composites

In the process of the formation of oil-absorbing resin, the content of hierarchical

$\text{Al}_2\text{O}_3$  clusters may play a critical role to form the 3D network structure and determine the oil absorption properties of porous  $\text{Al}_2\text{O}_3$ /acrylic resin composites, thereby it is necessary to discuss the effect of the modified  $\text{Al}_2\text{O}_3$  powder content on oil absorbency.  $Q_{\text{eq}}$  is the indicator of oil absorbency and all result of the oil adsorption amount of the different modified  $\text{Al}_2\text{O}_3$  powder content are showed in the Fig.9. As shown in the Fig.9, oil absorbency varies with the modified  $\text{Al}_2\text{O}_3$  power content. For carbon tetrachloride, the absorption properties of porous  $\text{Al}_2\text{O}_3$ /resin composites increase with increasing  $\text{Al}_2\text{O}_3$  clusters content, reaches a maximum absorption property of 30 g/g at the content of 3 wt%  $\text{Al}_2\text{O}_3$  clusters. It may be that hydrophobic modified  $\text{Al}_2\text{O}_3$  clusters dispersed in the resin has a certain supporting function for the 3D network structure and provides more space and channels for oil absorption. Whereas there is a decline in absorption properties for further increasing the  $\text{Al}_2\text{O}_3$  clusters content, because the excessive modified  $\gamma\text{-Al}_2\text{O}_3$  clusters may occupy the space of three-dimensional net structure and reduce the swelling properties of the resin by hinder the stretching of chains, which is not conducive to oil absorption. A similar trend is observed for the methylbenzene and edible oils absorption. Hence, the content of 3% hydrophobic modified  $\text{Al}_2\text{O}_3$  clusters has been chosen for further organic solvents and oils absorption experiments. It is noteworthy that the carbon tetrachloride absorption property of porous  $\text{Al}_2\text{O}_3$ /acrylic resin composites is higher than that of methylbenzene, because of the higher density and the smaller polar molecules of carbon tetrachloride. However, the edible oils absorption of porous  $\text{Al}_2\text{O}_3$ /acrylic resin composites is the lowest. This may be because the self-swelling

properties of porous  $\text{Al}_2\text{O}_3$ /acrylic resin composites are more preferably in small molecule solvents.

It is extremely to measure the absorption properties of the porous  $\text{Al}_2\text{O}_3$ /acrylic resin composites. Six kinds of frequently encountered organic solvents and oils, namely dimethylformamide (DMF), edible oils,  $\text{CCl}_4$ ,  $\text{CHCl}_3$ , engine oil, and toluene, were used to evaluate the absorption properties of porous  $\text{Al}_2\text{O}_3$ /acrylic resin composites, and the results are shown in Fig. 10. The porous  $\text{Al}_2\text{O}_3$ /acrylic resin composites show high absorbency for these oils and organic solvents. In general, the oil absorptions of the porous  $\text{Al}_2\text{O}_3$ /acrylic resin composites were 6.8-30.1 times its own weight and this is significantly superior to carbon nanotubes/polyurethane foam and oil absorption resins [25, 38].

To demonstrate the feasibility of the porous  $\text{Al}_2\text{O}_3$ /acrylic resin composites in the organic solvents absorption, the toluene dyed with Sudan III was selected as the representative absorbate on behalf of organic solvents in the performance of the removal of oils and organic solvents from water. As shown in Fig. 11, a piece of resin composites was immersed into the mixture with several drops of toluene floating on the surface of water. It was observed to float on the mixture and absorb organic liquid rapidly without leaving a trace within ten minutes, indicating the high oil-absorbing ability of the porous  $\text{Al}_2\text{O}_3$  resin composites. This commendable property indicated the possibility for environmental applications to remove organic liquid from water.

### 3.5 Reusability and oil retention capacity of resin composites

Reusability of oil-absorbents is a significant property for oil separation in

practical application. In order to evaluate the reusability of the porous  $\text{Al}_2\text{O}_3$ /acrylic resin composites, the as-synthesized resin composites were immersed in organic solvents for saturated absorption. Oil absorption capacities of resin composites after five cycles of the sorption process for carbon tetrachloride and methylbenzene are shown in Fig.12A. It was observed that with the increase of repetitions, the oil removal efficiency of resin composites decreased quite slowly. Even after five sorption cycles, the decrease in sorption capacity did not exceed 3% for carbon tetrachloride and 4% for methylbenzene, which may be not only the mild procedure without severe disruption of the materials to remove the absorbed organic solvents by the extraction of anhydrous ethanol, but also the robust three-dimensional network structure of resin composites. Fig.12B shows the excellent oil retention capacity of resin composites compared with traditional oil absorption materials including bamboo fiber, straw and clay. In experiment, these materials were weighed and immersed in the toluene for 2h. Then, the oil absorption materials were taken out from the solution and weighed for pre-set time intervals. Thus, the resin composites with high oil-absorbing ability, the excellent recyclability and high oil retention capacity have admirable potential application in oils and organic solvents absorption.

#### 4. Conclusions

In summary, an all-around oil-absorbing material composed of hierarchical  $\text{Al}_2\text{O}_3$  clusters and acrylic resin by combined hydrothermal method and suspension polymerization method. The hierarchical porous  $\text{AlOOH}$  had been synthesized by a simple hydrothermal method and  $\text{Al}_2\text{O}_3$  nanomaterial obtained by calcining  $\text{AlOOH}$

remained the unique structure of AlOOH. To enhance the hydrophobic and oleophilic properties, silane coupling agent A151 was used to modify the surface of hierarchical Al<sub>2</sub>O<sub>3</sub> clusters. With the help of A151, the wettability of Al<sub>2</sub>O<sub>3</sub> obtained by calcining AlOOH was changed. The relevant results disclosed that the hydrophobic groups were successfully grafted on the surfaces of hierarchical Al<sub>2</sub>O<sub>3</sub> clusters with water contact angle of 145.49°. By utilizing suspension polymerization method, the porous Al<sub>2</sub>O<sub>3</sub>/acrylic resin composites were fabricated by the polymerization of the MBA, BA and modified hierarchical Al<sub>2</sub>O<sub>3</sub> clusters under microwave irradiation. The TG-DSC results indicated that the thermal stability of resin composites was improved by introduction of hierarchical Al<sub>2</sub>O<sub>3</sub> clusters. It was found that the resin composites have a high absorbency, 30 g/g for carbon tetrachloride, 7 g/g for edible oils and 18 g/g for methylbenzene. Even more excitingly, the resin composites exhibited excellent oil absorption properties and the excellent recyclability. Moreover, the high oil retention capacities of resin composites were also demonstrated. The as-synthesized resin composites can work as an efficient and durable oil-absorbing material for the separation of organic solvent. These outstanding performances endow the material to be an ideal candidate to separate oils and organic solvents from water.

### **Acknowledgments**

The National Natural Science Foundation of China (U1507115 and 21576120), Natural Science Foundation of Jiangsu Province (BK20160500, BK20161362 and BK20160774), Postdoctoral Science Foundation of Jiangsu Province (1601016A), and Scientific Research Foundation for Advanced Talents, Jiangsu University (15JDG142)

are thanked for their financial support.

## References

- [1] D. Sidiras, F. Batzias, I. Konstantinou, M. Tsapatsis, Simulation of autohydrolysis effect on adsorptivity of wheat straw in the case of oil spill cleaning, *Chem. Eng. Res. Des.* 92 (2014) 1781-1791.
- [2] T. Mohammadi, A. Esmaelifar, Wastewater treatment of a vegetable oil factory by a hybrid ultrafiltration-activated carbon process, *J. Membr. Sci.* 254 (2005) 129-137.
- [3] P. Li, B. Yu, X. Wei, Synthesis and characterization of a high oil $\square$ absorbing magnetic composite material, *J. Appl. Polym. Sci.* 93 (2004) 894-900.
- [4] S. Wang, K. Liu, X. Yao, L. Jiang, Bioinspired surfaces with superwettability: new insight on theory, design, and applications, *Chem. Rev.* 115 (2015) 8230-8293.
- [5] J. Zhao, Y. Xue, R. Qiu, W. Guo, L. Fan, P. Wang, Superoleophilic *Ulva prolifera* for oil/water separation: A repayment from the green tide, *Chem. Eng. J.* 292 (2016) 147-155.
- [6] J. Li, C. Xu, Y. Zhang, R. Wang, F. Zha, H. She, Robust superhydrophobic attapulgite coated polyurethane sponge for efficient immiscible oil/water mixture and emulsion separation, *J. Mate. Chem. A* (2016).
- [7] C. Zhou, J. Cheng, K. Hou, A. Zhao, P. Pi, X. Wen, S. Xu, Superhydrophilic and underwater superoleophobic titania nanowires surface for oil repellency and oil/water separation, *Chem. Eng. J.* 301 (2016) 249-256.

- [8] T. Zhang, L. Kong, M. Zhang, F. Qiu, J. Rong, J. Pan, Synthesis and characterization of porous fibers/polyurethane foam composites for selective removal of oils and organic solvents from water, *RSC Adv.* 6 (2016) 86510-86519.
- [9] J. Li, L. Yan, X. Tang, H. Feng, D. Hu, F. Zha, Robust Superhydrophobic Fabric Bag Filled with Polyurethane Sponges Used for Vacuum-Assisted Continuous and Ultrafast Absorption and Collection of Oils from Water, *Adv. Mater. Interfaces.* 3 (2016), Doi:10.1039/C6TA07535E.
- [10] M.A. Zahed, H.A. Aziz, M.H. Isa, L. Mohajeri, S. Mohajeri, Optimal conditions for bioremediation of oily seawater, *Bioresour. Technol.* 101 (2010) 9455-9460.
- [11] S.L. Bacon, A.J. Daugulis, J.S. Parent, Effect of polymer molecular weight distribution on solute sequestration in two-phase partitioning bioreactors, *Chem. Eng. J.* 299 (2016) 56-62.
- [12] D. Tian, X. Zhang, X. Wang, J. Zhai, L. Jiang, Micro/nanoscale hierarchical structured ZnO mesh film for separation of water and oil, *Phys. Chem. Chem. Phys.* 13 (2011) 14606-14610.
- [13] J. Li, L. Yan, Y. Zhao, F. Zha, Q. Wang, Z. Lei, One-step fabrication of robust fabrics with both-faced superhydrophobicity for the separation and capture of oil from water, *Phys. Chem. Chem. Phys.* 17 (2015) 6451-6457.Y.

- [14] Y. Chen, B. Yu, J. Lin, R. Naidu, Z. Chen, Simultaneous adsorption and biodegradation (SAB) of diesel oil using immobilized *Acinetobacter venetianus* on porous material, *Chem. Eng. J.* 289 (2016) 463-470.
- [15] A. Pavía-Sanders, S. Zhang, J.A. Flores, J.E. Sanders, J.E. Raymond, K.L. Wooley, Robust magnetic/polymer hybrid nanoparticles designed for crude oil entrapment and recovery in aqueous environments, *ACS Nano* 7 (2013) 7552-7561.
- [16] W. Liang, Y. Liu, H. Sun, Z. Zhu, X. Zhao, A. Li, W. Deng, Robust and all-inorganic absorbent based on natural clay nanocrystals with tunable surface wettability for separation and selective absorption, *RSC Adv.* 4 (2014) 12590-12595.
- [17] J. Jang, B.-S. Kim, Studies of crosslinked styrene-alkyl acrylate copolymers for oil absorbency application. I. Synthesis and characterization, *J. Appl. Polym. Sci.* 77 (2000) 903-913.
- [18] S. Salem, A. Salem, A. Agha Babaei, Preparation and characterization of nano porous bentonite for regeneration of semi-treated waste engine oil: Applied aspects for enhanced recovery, *Chem. Eng. J.* 260 (2015) 368-376.
- [19] Y. Gao, D. Zhao, M.-W. Chang, Z. Ahmad, J.-S. Li, Optimising the shell thickness-to-radius ratio for the fabrication of oil-encapsulated polymeric microspheres, *Chem. Eng. J.* 284 (2016) 963-971.



- [20]S. Ibrahim, S. Wang, H.M. Ang, Removal of emulsified oil from oily wastewater using agricultural waste barley straw, *Biochem. Eng. J.* 49 (2010) 78-83.
- [21]H.M. Choi, R.M. Cloud, Natural sorbents in oil spill cleanup, *Environ. Sci. Technol.* 26 (1992) 772-776.
- [22]J. Jang, B.-S. Kim, Studies of crosslinked styrene-alkyl acrylate copolymers for oil absorbency application. I. Synthesis and characterization, *J. Appl. Polym. Sci.* 77 (2000) 903-913.
- [23]T. Zhang, Q. Zhang, X. Wang, Q. Li, J. Rong, F. Qiu, Synthesis of  $Mn_2O_3$ /poly(styrene-co-butyl methacrylate) resin composites and their oil-absorbing properties, *RSC Advances* 5 (2015) 101186-101192.
- [24]H.Z. Mei, W.J. Cho, Synthesis and properties of high oil-absorbent 4-*tert*-butylstyrene-EPDM-divinylbenzene graft terpolymer, *J. Appl. Polym. Sci.* 85 (2002) 2119-2129.
- [25]X.M. Zhou, C.Z. Chuai, Synthesis and characterization of a novel high-oil-absorbing resin, *J. Appl. Polym. Sci.* 115 (2010) 3321-3325.
- [26]G.-R. Shan, P.-Y. Xu, Z.-X. Weng, Z.-M. Huang, Synthesis and properties of oil absorption resins filled with polybutadiene, *J. Appl. Polym. Sci.* 89 (2003) 3309-3314.
- [27]M.E. Wright, D.A. Schorzman, F.J. Feher, R.-Z. Jin, Synthesis and thermal curing of Aryl-Ethynyl-Terminated co POSS imide oligomers: new inorganic/organic hybrid resins, *Chem. Mater.* 15 (2003) 264-268.

- [28] B.P. Tripathi, V.K. Shahi, Organic-inorganic nanocomposite polymer electrolyte membranes for fuel cell applications, *Prog. Polym. Sci.* 36 (2011) 945-979.
- [29] T. Zhang, L. Kong, Y. Dai, X. Yue, J. Rong, F. Qiu, J. Pan, Enhanced oils and organic solvents absorption by polyurethane foams composites modified with MnO<sub>2</sub> nanowires, *Chem. Eng. J.* doi.org/10.1016/j.cej.2016.08.085.
- [30] S. Wilson, The dehydration of boehmite,  $\gamma$ -AlOOH, to  $\gamma$ -Al<sub>2</sub>O<sub>3</sub>, *J. Hazard. Mater.* 30 (1979) 247-255.
- [31] G.R. Shan, P.Y. Xu, Z.X. Weng, Z.M. Huang, Oil-absorption function of physical crosslinking in the high-oil-absorption resins, *J. Hazard. Mater.* 90 (2003) 3945-3950.
- [32] A. Dandapat, D. Jana, G. De, Synthesis of thick mesoporous gamma-alumina films, loading of Pt nanoparticles, and use of the composite film as a reusable catalyst, *ACS Appl. Mater. Interfaces* 1 (2009) 833-840.
- [33] X.Y. Chen, H.S. Huh, S.W. Lee, Hydrothermal synthesis of boehmite ( $\gamma$ -AlOOH) nanoplatelets and nanowires: pH-controlled morphologies, *Nanotechnology* 18 (2007) 1107-1110.
- [34] T.-Z. Ren, Z.-Y. Yuan, B.-L. Su, Microwave-assisted preparation of hierarchical mesoporous-macroporous boehmite AlOOH and  $\gamma$ -Al<sub>2</sub>O<sub>3</sub>, *Langmuir* 20 (2004) 1531-1534.
- [35] J.Y. Xiang, J.P. Tu, L. Zhang, Y. Zhou, X.L. Wang, S.J. Shi, Simple synthesis of surface-modified hierarchical copper oxide spheres with needle-like

morphology as anode for lithium ion batteries, *Electrochim. Acta* 55 (2010) 1820-1824.

[36]C.H. Shek, J.K.L. Lai, T.S. Gu, G.M. Lin, Transformation evolution and infrared absorption spectra of amorphous and crystalline nano- $\text{Al}_2\text{O}_3$  powders, *Nanostruct. Mater.* 8 (1997) 605-610.

[37]C.H. Shek, J.K.L. Lai, T.S. Gu, G.M. Lin, Transformation evolution and infrared absorption spectra of amorphous and crystalline nano- $\text{Al}_2\text{O}_3$  powders, *Nanostruct. Mater.* 8 (1997) 605-610.

[38]A. Keshavarz, H. Zilouei, A. Abdolmaleki, A. Asadinezhad, Enhancing oil removal from water by immobilizing multi-wall carbon nanotubes on the surface of polyurethane foam, *J. Environ. Manage.* 157 (2015) 279-286.

**Figure captions:**

Scheme 1. Schematic illustration for surface modification of hierarchical porous  $\text{Al}_2\text{O}_3$ .

Scheme 2. Schematic illustration for porous  $\text{Al}_2\text{O}_3$ /acrylic resin composites.

Fig.1 XRD patterns of  $\gamma$ - $\text{AlOOH}$  (a) and  $\gamma$ - $\text{Al}_2\text{O}_3$  (b).

Fig.2 (A) Low- and (B) high-magnification SEM images of  $\text{Al}_2\text{O}_3$ .

Fig.3 Nitrogen absorption and desorption isotherms and pore size distribution (inset) of the obtained  $\text{Al}_2\text{O}_3$  clusters.

Fig. 4 Water contact angle measurements for prepared  $\text{Al}_2\text{O}_3$  (A) and modified  $\text{Al}_2\text{O}_3$  (B).

Fig. 5 Dynamic absorbing process of water on the modified  $\text{Al}_2\text{O}_3$  powder.

Fig. 6 FT-IR spectra of hierarchical porous  $\text{Al}_2\text{O}_3$  clusters (A, unmodified; B, modified).

Fig. 7 SEM images of raw acrylic ester resin (A) and resin composites (B).

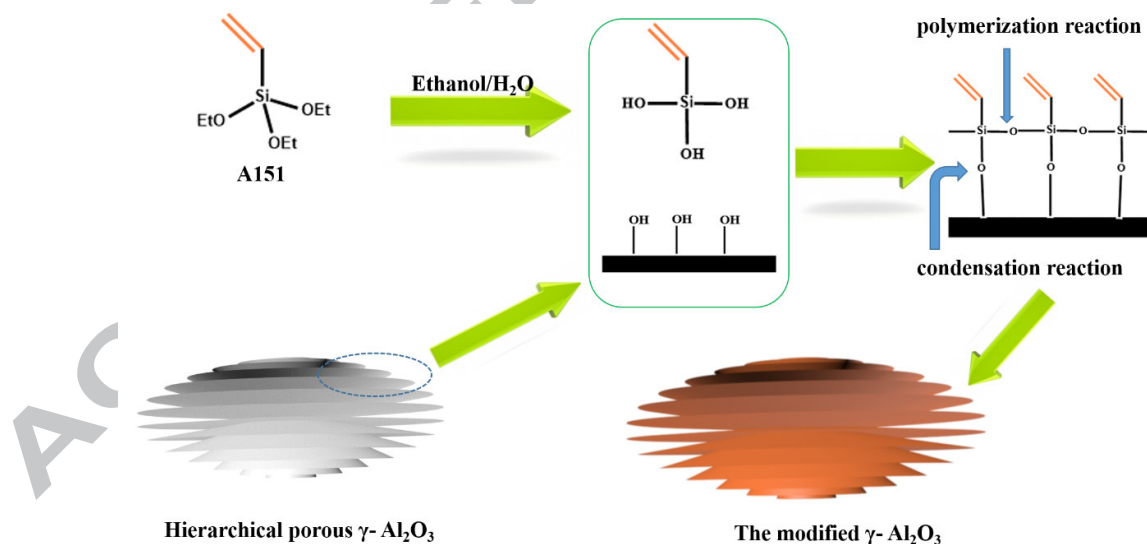
Fig.8 TG-DSC curves for acrylic ester resin (A) and  $\gamma$ - $\text{Al}_2\text{O}_3$  resin composites (B).

Fig.9 Effect of the modified  $\text{Al}_2\text{O}_3$  powder content on oil absorbency.

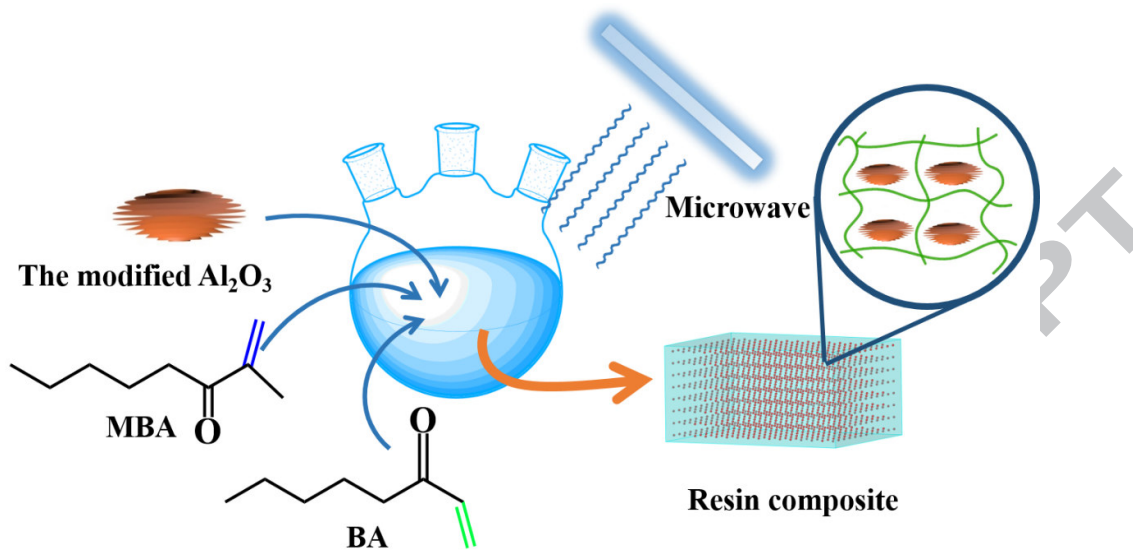
Fig.10. Absorbency of the porous  $\text{Al}_2\text{O}_3$ /acrylic resin composites for organics.

Fig.11. Removing toluene droplets (labelled with oil Sudan III dye) from the surface of water using the  $\text{Al}_2\text{O}_3$  resin composites.

Fig.12 Reusability (A) and oil retention capacity (B) of the porous  $\text{Al}_2\text{O}_3$ /acrylic resin composites.



Scheme 1. Schematic illustration for surface modification of hierarchical porous  $\text{Al}_2\text{O}_3$



Scheme 2. Schematic illustration for porous  $\text{Al}_2\text{O}_3$ /acrylic resin composites.

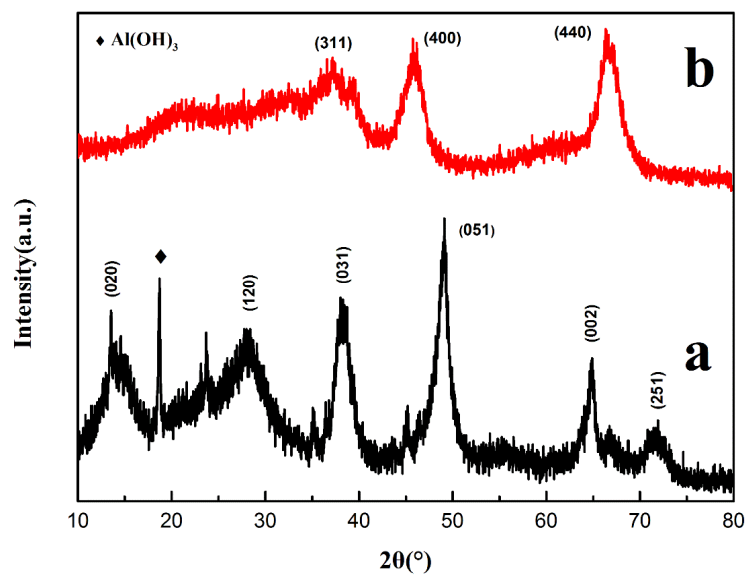


Fig.1 XRD patterns of  $\gamma\text{-AlOOH}$  (a) and  $\gamma\text{-Al}_2\text{O}_3$  (b).

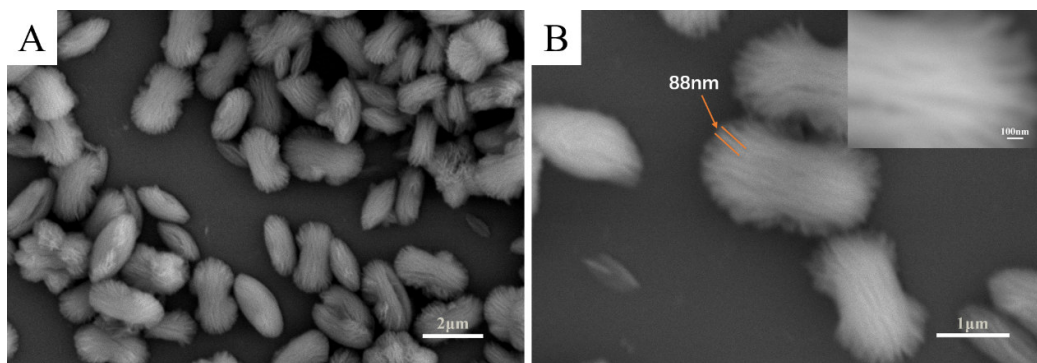


Fig.2 (A) Low- and (B) high-magnification SEM images of  $\text{Al}_2\text{O}_3$ .

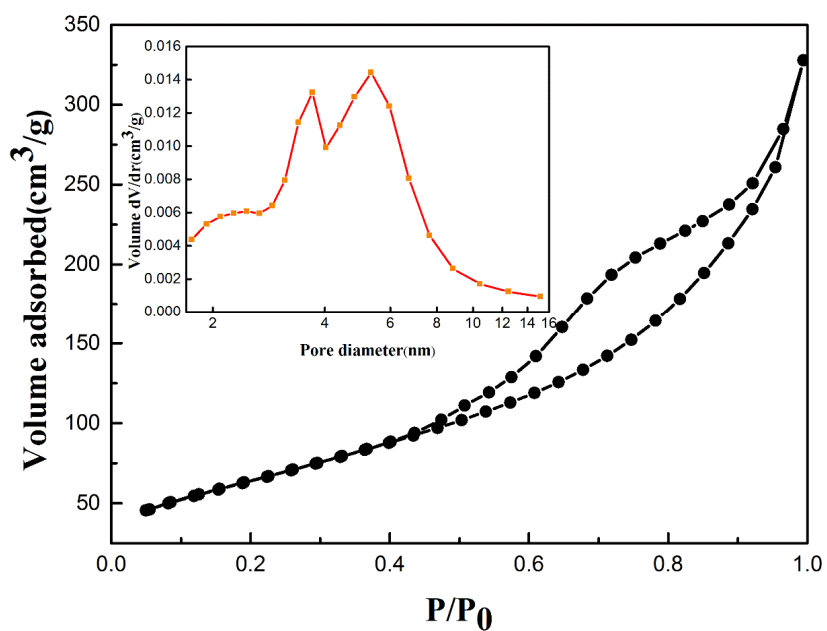


Fig.3 Nitrogen adsorption and desorption isotherms and pore size distribution (inset) of the obtained  $\text{Al}_2\text{O}_3$  clusters.

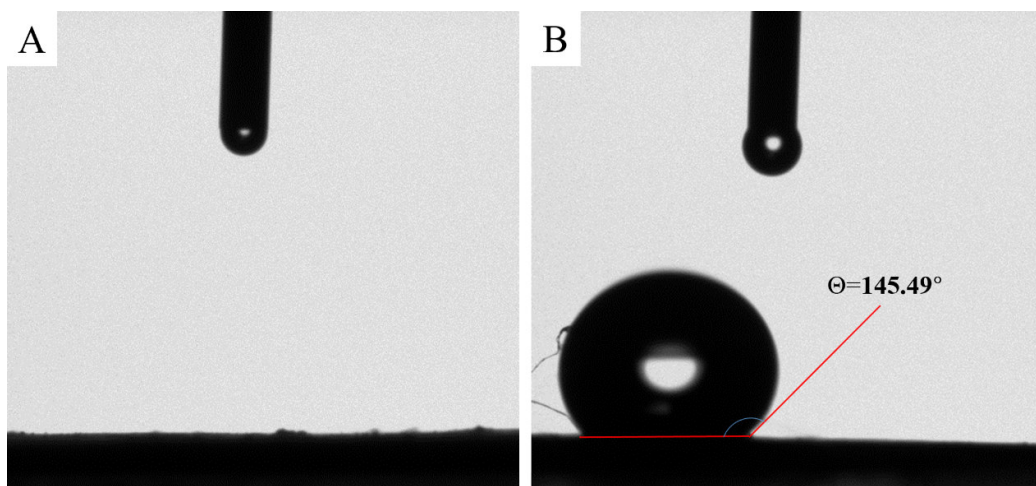


Fig. 4 Water contact angle measurements for porous Al<sub>2</sub>O<sub>3</sub> (A) and modified Al<sub>2</sub>O<sub>3</sub> (B).

ACCEPTED MANUSCRIPT

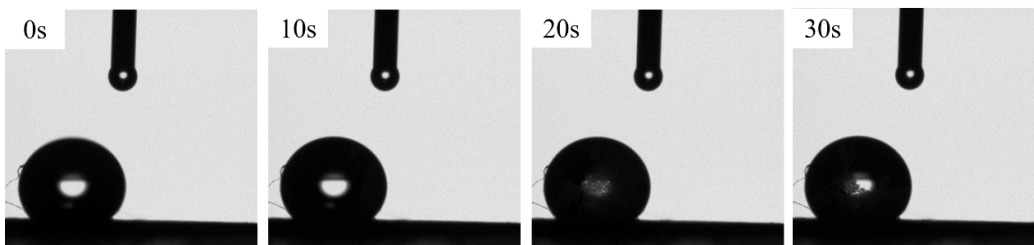


Fig. 5 Dynamic absorbing process of water on the modified  $\text{Al}_2\text{O}_3$  powder.

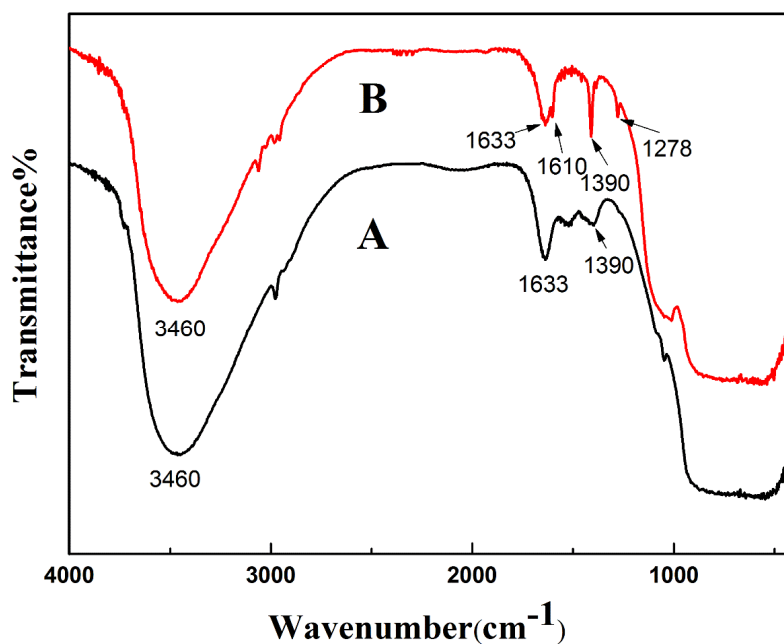


Fig. 6 FT-IR spectra of hierarchical porous  $\text{Al}_2\text{O}_3$  clusters (A, unmodified; B, modified).



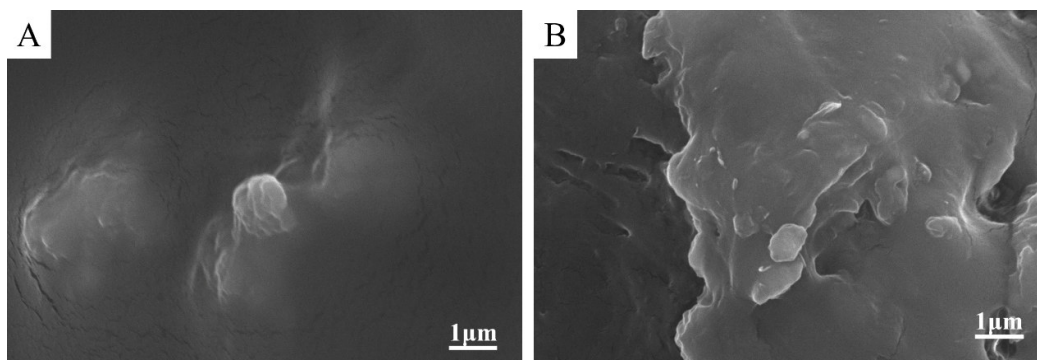


Fig. 7 SEM images of raw acrylic ester resin (A) and resin composites (B).

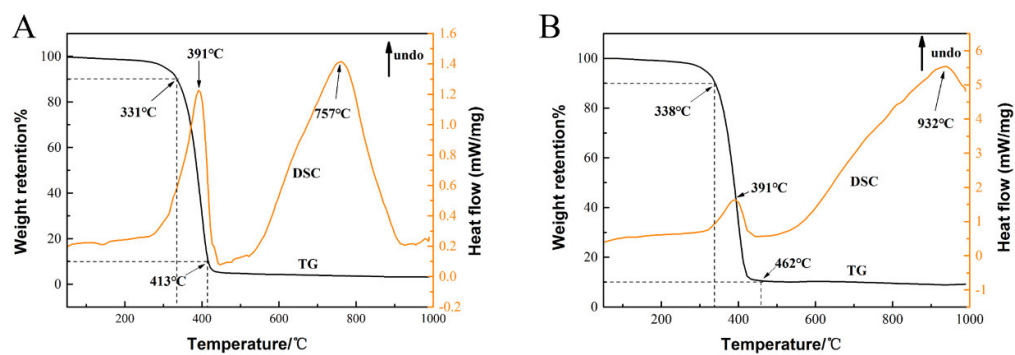


Fig.8 TG-DSC curves for acrylic ester resin (A) and Al<sub>2</sub>O<sub>3</sub> resin composites (B).

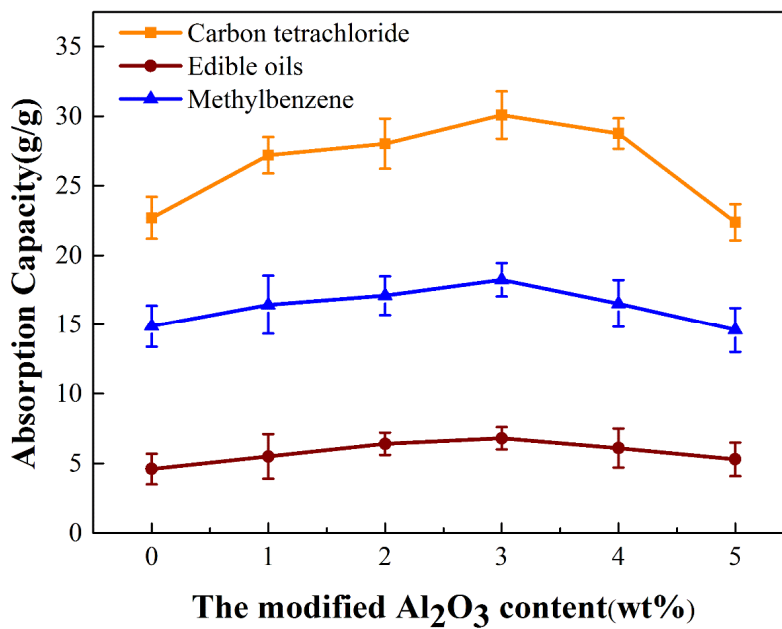


Fig.9 Effect of the modified  $\text{Al}_2\text{O}_3$  powder content on oil absorbency.

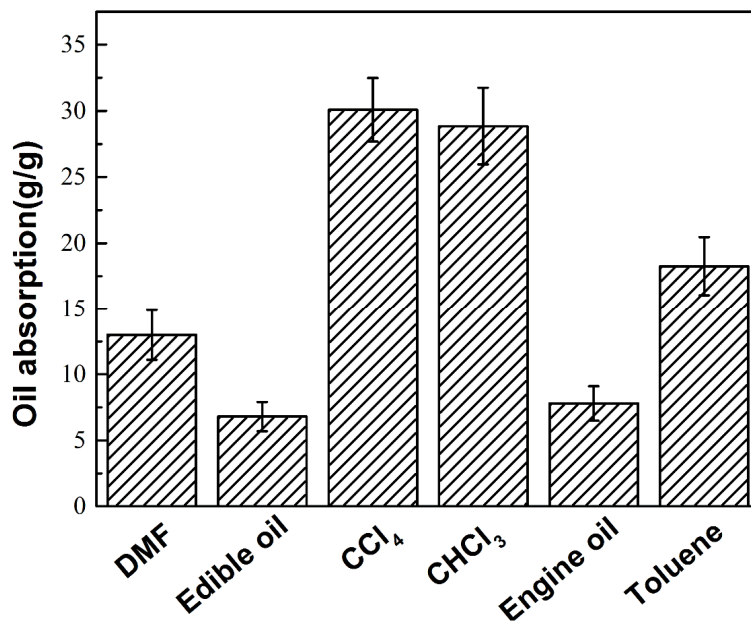


Fig.10. Absorbency of the porous  $\text{Al}_2\text{O}_3$ /acrylic resin composites for organics.

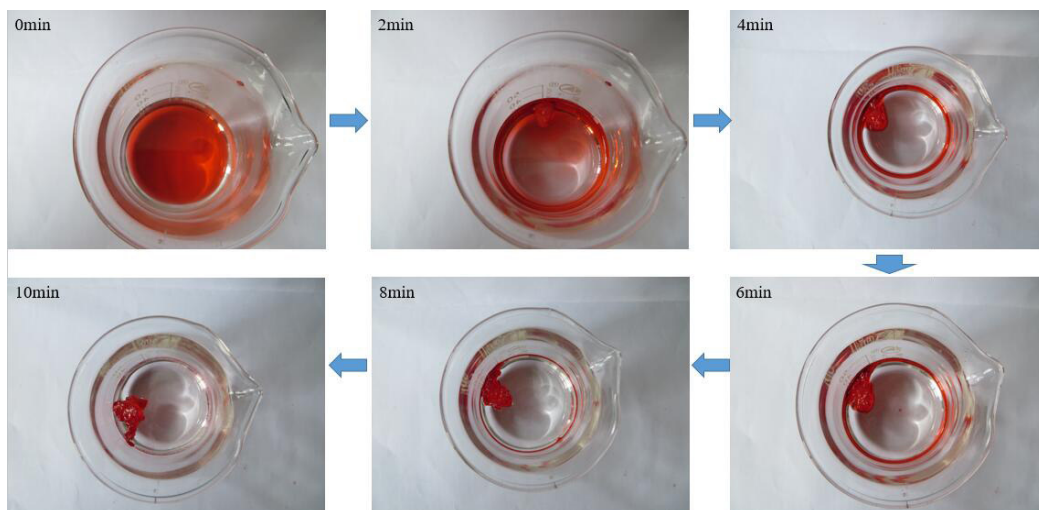


Fig.11. Removing toluene droplets (labelled with oil Sudan III dye) from the surface of water using the  $\text{Al}_2\text{O}_3$  resin composites.

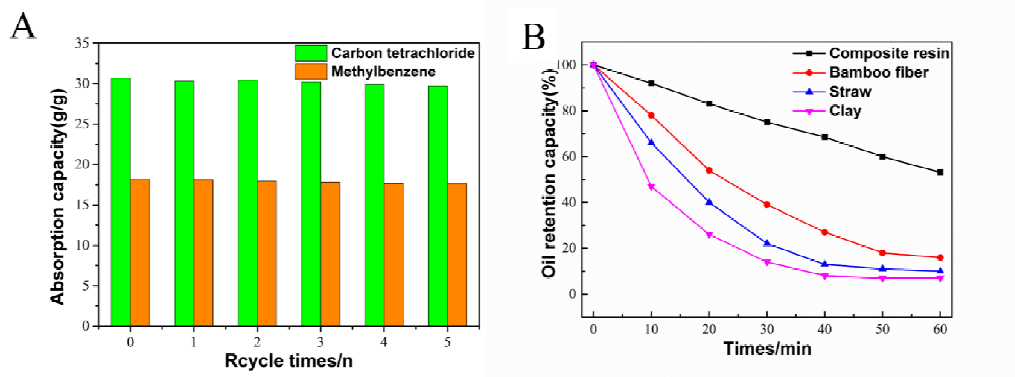
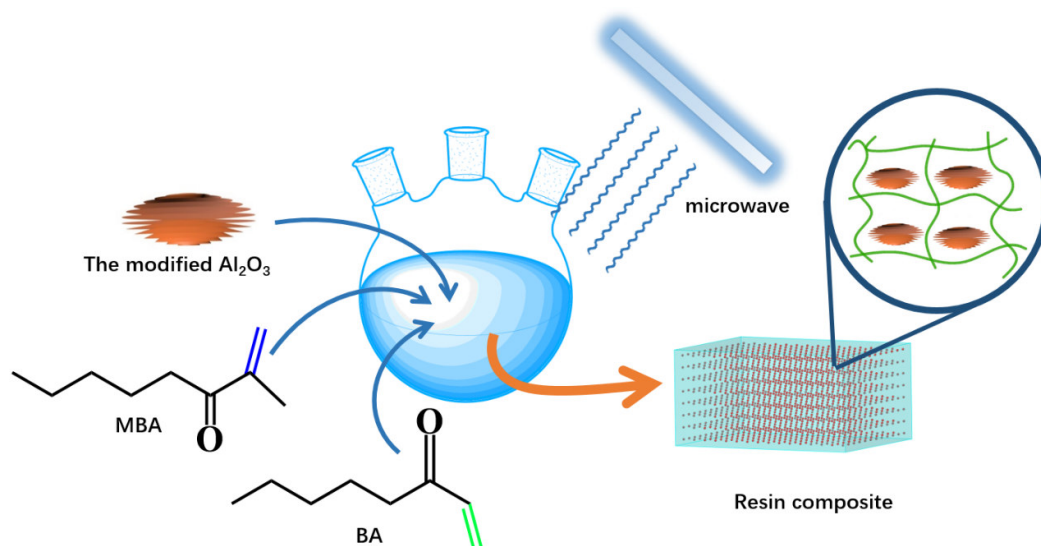


Fig.12 Reusability (A) and oil retention capacity (B) of the porous  $\text{Al}_2\text{O}_3$ /acrylic resin composites.



ACCEPTED MANUSCRIPT

**Highlights**

- Hierarchical Al<sub>2</sub>O<sub>3</sub> was prepared by using CTAB as a structure-directing agent.
- Resin composites were synthesized by suspension polymerization.
- The oil absorption properties are affected by the content of Al<sub>2</sub>O<sub>3</sub>.
- Porous resin composites exhibited high oils absorption properties.
- Oil absorbency and thermal stability of the composite resin were improved.